nature biomedical engineering

Article

https://doi.org/10.1038/s41551-023-01138-7

Week-long norm glycaemia in diabetic mice and minipigs via a subcutaneous dose of a glucose-responsive insulin complex

Received: 25 August 2022

Accepted: 17 October 2023

Published online: 06 December 2023

Check for updates

Juan Zhang[1,2,3], Xiangqian Wei[1,2,3], Wei Liu[1,2,3], Yanfang Wang[1,2,3], Anna R. Kahkoska[4], Xianchi Zhou[5], Huimin Zheng[1], Wentao Zhang[1,2,3], Tao Sheng[1,2,3], Yang Zhang[1,2,3], Yun Liu[1,2,3], Kangfan Ji[1,2,3], Yichen Xu[1,6], Peng Zhang[5], Jianchang Xu[1,2,3], John. B. Buse[7], Jinqiang Wang[1,2,6] ✉ & Zhen Gu[1,2,3,5,8,9] ✉

Glucose-responsive formulations of insulin can increase its therapeutic index and reduce the burden of its administration. However, it has been difficult to develop single-dosage formulations that can release insulin in both a sustained and glucose-responsive manner. Here we report the development of a subcutaneously injected glucose-responsive formulation that nearly does not trigger the formation of a fibrous capsule and that leads to week-long normoglycaemia and negligible hypoglycaemia in mice and minipigs with type 1 diabetes. The formulation consists of gluconic acid-modified recombinant human insulin binding tightly to poly-L-lysine modified by 4-carboxy-3-fluorophenylboronic acid via glucose-responsive phenylboronic acid–diol complexation and electrostatic attraction. When the insulin complex is exposed to high glucose concentrations, the phenylboronic acid moieties of the polymers bind rapidly to glucose, breaking the complexation and reducing the polymers' positive charge density, which promotes the release of insulin. The therapeutic performance of this long-acting single-dose formulation supports its further evaluation and clinical translational studies.

Diabetes mellitus is a chronic disease that affects more than 537 million adults worldwide. More than 20% of people with diabetes require insulin replacement therapy to maintain blood glucose (BG) levels within the normal range[1–3]. A number of different insulin formulations and delivery modalities have been developed to improve BG management. For example, the combination of long-acting 'basal' insulin with 'boluses' of rapid-acting insulin with meals is an effective regimen for maintaining both fasting and postprandial glucose within normal ranges. Yet, insulin therapy is burdensome because it requires multiple subcutaneous injections per day[4]. Moreover, insulin needs are

[1]National Key Laboratory of Advanced Drug Delivery and Release Systems, College of Pharmaceutical Sciences, Zhejiang University, Hangzhou, China. [2]Jinhua Institute of Zhejiang University, Jinhua, China. [3]Key Laboratory of Advanced Drug Delivery Systems of Zhejiang Province, College of Pharmaceutical Sciences, Zhejiang University, Hangzhou, China. [4]Department of Nutrition, University of North Carolina at Chapel Hill, Chapel Hill, NC, USA. [5]MOE Key Laboratory of Macromolecule Synthesis and Functionalization of Ministry of Education, Department of Polymer Science and Engineering, Zhejiang University, Hangzhou, China. [6]Department of Pharmacy, Second Affiliated Hospital, Zhejiang University School of Medicine, Zhejiang University, Hangzhou, China. [7]Department of Medicine, University of North Carolina School of Medicine, Chapel Hill, NC, USA. [8]Department of General Surgery, Sir Run Run Shaw Hospital, School of Medicine, Zhejiang University, Hangzhou, China. [9]Liangzhu Laboratory, Hangzhou, China. ✉e-mail: jinqiang_wang@zju.edu.cn; guzhen@zju.edu.cn

affected by a range of physiological and environmental factors; thus, dosing insulin accurately is challenging for people with diabetes and insulin therapy can be associated with a tremendous amount of hyper- and hypoglycaemia during the day and overnight[5]. New strategies for insulin delivery that effectively regulate BG, but with reduced injection frequency, are urgently needed.

Glucose-responsive insulin (GRI) can mimic β cell function by dynamically releasing insulin in response to changing BG; this approach to insulin therapy thus represents a promising alternative to the insulin formulations that are currently available[6–11]. GRI senses BG fluctuation and dynamically adjusts insulin release rates to modulate blood insulin levels and thus regulate BG in real time[12]. The dynamic component of GRI can expand the therapeutic index of insulin, reducing both hyper- and hypoglycaemia episodes that occur in an unreasonable insulin administration dose. Three glucose-responsive mechanisms, phenylboronic acid (PBA) derivatives[13–28], glucose-binding molecules[29–31] and glucose oxidase[32–40], have been extensively explored to construct GRI. Of these, the PBA-based GRI has progressed rapidly and has the potential for clinical applications based on rapid and robust in vitro and in vivo GRI release performance[27,28]. However, it remains a challenge to formulate a GRI that can regulate BG within the normal ranges for longer than one week after administration of a single dose, which requires the insulin formulation to simultaneously possess the capacity for fast postprandial insulin release and continuous, sustained 'basal' insulin release.

Here we describe a glucose-responsive formulation of insulin that achieves both GRI release and long-acting performance (Fig. 1a). In this formulation, recombinant human insulin is covalently modified with gluconic acid to generate an insulin analogue with a diol moiety (Glu-insulin). Glu-insulin can form a stable complex with 4-carboxy-3-fluorobenzeneboronic acid (FPBA)-modified poly-L-lysine (PLL-FPBA) through dynamic electrostatic attraction and PBA–diol complexation. In the normoglycaemic condition, both the strong electrostatic force and the PBA–diol complexation cause the complex formulation to release an ultra-small amount of insulin in a free state, providing slow and continuous insulin release and allowing for a high dose. Under the hyperglycaemic condition, the binding of glucose to FPBA moieties instantly reduces the positive charge density of PLL-FPBA and deconstructs phenylboronate ester bonds, therefore reducing the electrostatic attractions and the density of phenylboronate ester bonds between Glu-insulin and polymers, and eventually promoting insulin release. In the chemically induced type 1 diabetic mouse model, the subcutaneously injected insulin complex forms a depot under the skin, maintaining blood insulin levels at a steady 'basal' level and BG levels within a normal range. Upon glucose administration, the elevated BG triggers fast insulin release from the complex depot, correcting elevated BG levels. As BG returns to a normal range, the decreasing BG provides a negative feedback signal to the complex to reduce the insulin release rate. Of note, the complex is fibrous capsule resistant, which is essential for the long-acting component of insulin release from the complex depot. This GRI can achieve week-long normoglycaemia following administration, with minimal hypoglycaemia incidence. In addition, anti-hyperglycaemic effects were observed for more than 20 days, even though the steadily reduced amount of insulin depot under the skin is not enough to maintain the BG below the normal level after one week posttreatment. The therapeutic efficacy of the GRI was further validated in type 1 diabetic minipigs.

Results

PLL-FPBA was previously reported to have glucose-responsive properties and low toxicity[27] and was thus selected in this study. The PLL-FPBA used here had around 65% of the amino groups modified with FPBA as calculated from the ^{1}H NMR spectrum (Supplementary Fig. 1a). The molecular weight of PLL-FPBA is poly-dispersed (Supplementary Fig. 1b) and the presence of boron is confirmed by the ^{11}B NMR spectrum (Supplementary Fig. 1c). Glu-insulin was prepared according to previously reported methods[41]. The gluconic acid modification was validated by matrix-assisted laser desorption/ionization time-of-flight mass spectrometry (Supplementary Fig. 2a). Glu-insulin had gluconic acid conjugation at A1 (N terminus of the α chain) of the insulin molecule (Supplementary Fig. 2b,c) and showed similar activity to unmodified recombinant human insulin, as evaluated on HepG2 cells and in diabetic mice (Supplementary Fig. 2d–f).

Mixing acidic PLL-FPBA and Glu-insulin aqueous solution yielded a white precipitate after adjusting the pH to 7. Equal weights of PLL-FPBA and Glu-insulin formed a stable insulin complex with unbound Glu-insulin at a concentration lower than 50 μg ml^{-1}, indicating a loading efficiency above 95% (Supplementary Fig. 3a–c). Of note, PLL-FPBA did not interfere with the detection of Glu-insulin using the Bradford assay reagent (Supplementary Fig. 3d). The insulin complex was a flocculent precipitate (Fig. 1b). Complexation of Glu-insulin and PLL-FPBA was further validated by an overlap in the fluorescence from fluorescein isothiocyanate (FITC)-labelled Glu-insulin and cyanine 5 (Cy5)-labelled PLL-FPBA (Fig. 1c). As confirmed by scanning electronic microscopy (SEM) and transmission electron microscopy (TEM), the complex had porous and loose micro-structures to allow for fast glucose diffusion and exchange, which is critical for a rapid glucose-responsive performance (Fig. 1d).

Glucose-stimulated insulin release from the complex was evaluated in PBS buffer at pH 7.4 with four glucose concentrations (0, 100, 200 and 400 mg dl^{-1}) (Fig. 1e and Supplementary Fig. 3e). At 0 mg dl^{-1}, unbound insulin was maintained at an ultra-low level of around 10 μg ml^{-1} for 5 h. After increasing the glucose concentration to 100, 200 and 400 mg dl^{-1} (representing normoglycaemia, mild hyperglycaemia and extreme hyperglycaemia, respectively), unbound insulin levels increased to 19.5 ± 10.7, 32.1 ± 10.9 and 45.2 ± 14.8 μg ml^{-1} after 2 h incubation, at which time the unbound insulin levels reached thermodynamic equilibrium and remained unchanged. This glucose concentration-dependent increase in unbound insulin levels indicated that glucose weakened the attraction between Glu-insulin and

Fig. 1 | Dually glucose-responsive complex for insulin delivery. a, Schematic of complex formation and insulin release with dual glucose-responsive mechanisms. The negatively charged diol moiety-containing Glu-insulin and the positively charged PBA moiety-containing PLL-FPBA can form a complex through electrostatic attraction and PBA–diol binding. Upon exposure of the complex to a solution with a high level of glucose, binding of glucose to the FPBA moiety instantly reduces the positive charge density on PLL-FPBA and disrupts the PBA–diol bonds, resulting in immediate insulin release. **b**, Representative pictures of the complex. The complexes were prepared using FITC-labelled Glu-insulin (orange) and unlabelled PLL-FPBA, Cy5-labelled PLL-FPBA (blue) and unlabelled Glu-insulin, or FITC-labelled Glu-insulin and Cy5-labelled PLL-FPBA. Equal weights of Glu-insulin and PLL-FPBA were used. **c**, Representative fluorescence images of the complex. FITC-labelled Glu-insulin and Cy5-labelled PLL-FPBA are shown in green and red, respectively. Scale bars, 500 μm. **d**, Representative SEM (upper) and TEM (lower) images of insulin complex. **e**, GRI release from the complex when exposed to a solution containing 0 (black), 100 (green), 200 (blue) and 400 mg dl^{-1} glucose (red). Data points are means ± s.d. (n = 3). **f**, Pulsatile insulin release profile when the complex was alternatively exposed to 400 and 100 mg dl^{-1} glucose solution. Data points are means ± s.d. (n = 3). **g**, Cumulative insulin release from complexes that were exposed to a glucose solution containing 0, 100, 200 and 400 mg dl^{-1} glucose. The complexes were incubated in each solution for 10 min. Data points are means ± s.d. (n = 5). The statistical analysis utilized a one-tailed unpaired Student's t-test, with $^{*}P$ = 0.0128, $^{**}P$ = 0.0025 and $^{*}P$ = 0.0359 indicating statistical significance between the 400 and 100 mg dl^{-1} groups and $^{\#\#}P$ = 0.0031 indicating statistical significance between the 200 and 100 mg dl^{-1} groups in **e**. All P value analyses were performed in GraphPad Prism (v.8).

https://doi.org/10.1038/s41551-023-01138-7

PLL-FPBA. The kinetics of GRI release were also evaluated. After 0.2 and 1 h incubation, insulin complexes in 400 mg dl^{-1} glucose solution achieved unbound Glu-insulin levels of 21.4 ± 6.1 and 37.8 ± 6.1 μg ml^{-1} (Fig. 1e), which were more than twofold greater than the level noted in the 100 mg dl^{-1} glucose concentration, leading to a glucose stimulation index >2 (Supplementary Fig. 3f)[42,43]. Collectively, both kinetically and thermodynamically, the complex released insulin glucose responsively. Next, the complex was exposed to 100 or 400 mg dl^{-1} glucose solution, and a pulsatile insulin release profile was observed (Fig. 1f).

The gradual decrease in the amount of insulin over cycles may arise from the limited diffusion rate of insulin from the inner of the complex because centrifugation compacted the complex. The insulin release rate was also observed to increase steadily with exposure to gradually increased glucose concentrations (Fig. 1g).

The amount of insulin dissolved in an aqueous solution and the volume of depot both determine BG regulation capability. Insulin glargine has low solubility in PBS at pH 7.4 and thus can be used as a daily administrated insulin formulation. However, its solubility is not

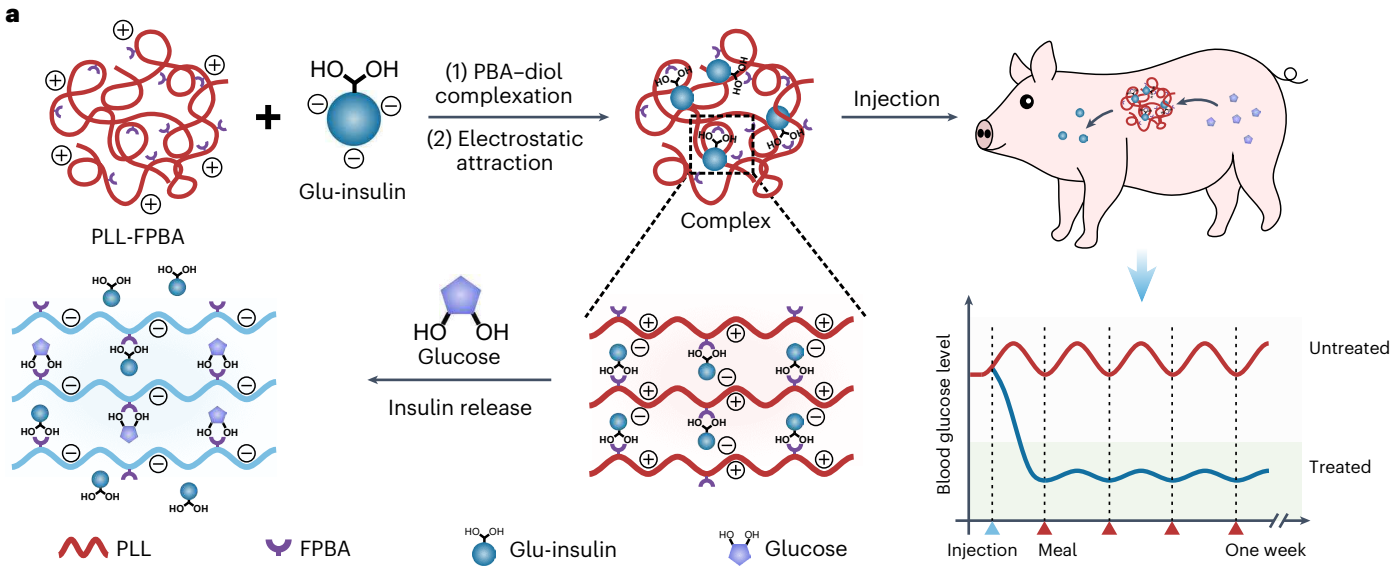

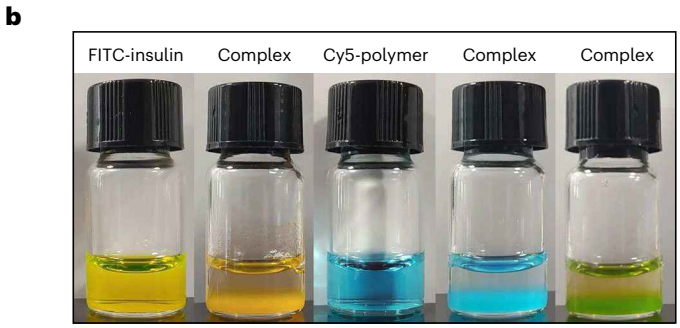

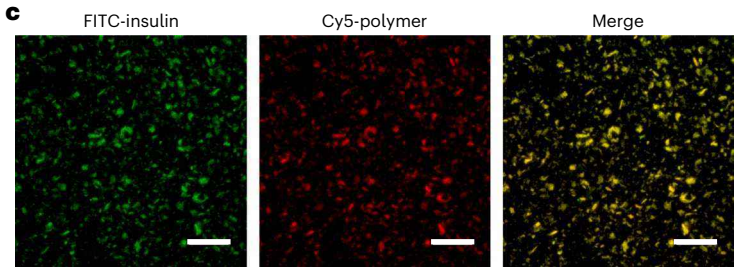

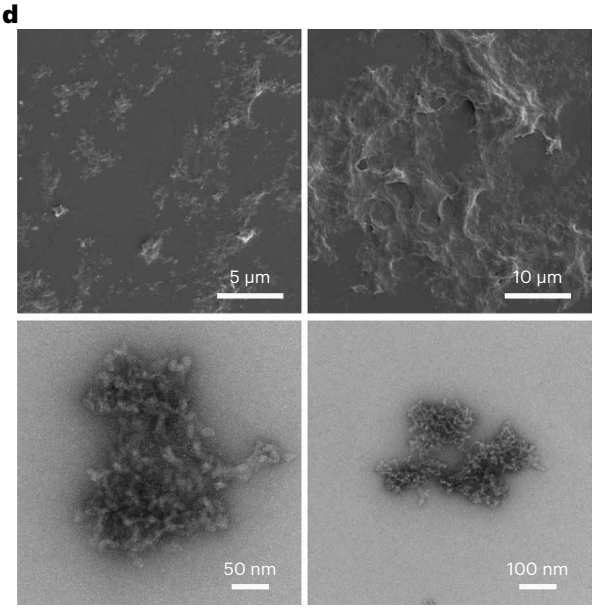

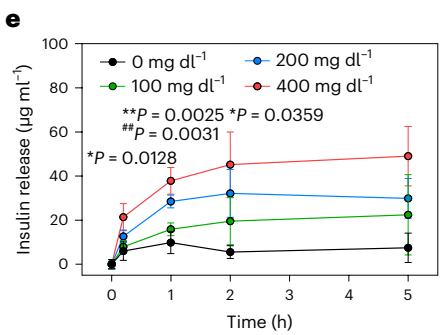

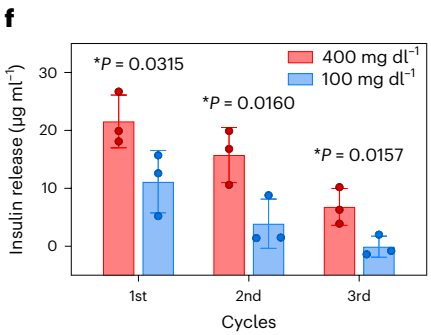

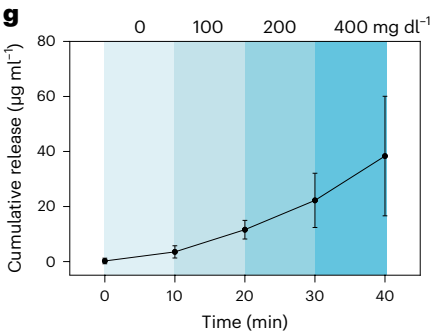

low enough for a weekly administrated formulation. Compared with insulin glargine[44], the insulin complex, with or without the presence of glucose, had even lower solubility in PBS at 7.4. This is essential for a high and safe dose, and accordingly the ultra-long BG-regulation ability of the insulin complex.

The mechanisms of insulin complex formation and insulin release were further studied. Succinic anhydride-modified insulin[45] did not form a stable complex with PLL-FPBA, indicating the necessity for diol moieties in Glu-insulin (Supplementary Fig. 4). We also prepared PLL-FPBA without residual amino groups (Supplementary Fig. 5), which did not form a complex with Glu-insulin either, suggesting the necessity of electrostatic attraction for complex formation. Thus, electrostatic attraction and PBA–diol complexation are essential to forming a complex with an ultra-low level of unbound insulin.

The insulin complex was evaluated in mice with type 1 diabetes induced by intraperitoneal streptozotocin (STZ) injection (150 mg kg^{-1}). Type 1 diabetic mice with fasting BG levels >300 mg dl^{-1} were selected to evaluate the treatment efficacy of the insulin complex. During treatment, mice had free access to food and water. The complex was studied preliminarily to determine the dose. After administration to diabetic mice at doses of 2.5, 5, 10 and 20 mg kg^{-1} (Extended Data Fig. 1), only the complex at the dose of 20 mg kg^{-1} achieved week-long normoglycaemia in mice. BG decreased rapidly to 99.0 ± 20.1 mg dl^{-1} in 1 h and remained almost unchanged during the first 8 h. Of note, the lowest BG of 74.2 ± 9.2 mg dl^{-1} was observed 4 h posttreatment (Extended Data Fig. 1d). Concurrently, the plasma insulin level was also measured using a human insulin enzyme-linked immunosorbent assay (ELISA) kit (Invitrogen). Plasma insulin peaked at 6 h posttreatment at 158.5 ± 9.5 μU ml^{-1} and then steadily decreased to 11.1 ± 6.0 μU ml^{-1} by 7 days posttreatment (Supplementary Fig. 6). As a result, a dose of 20 mg kg^{-1} was used in subsequent studies for comparison. The treatment efficacy of insulin complex and insulin glargine (Lantus, U-100) was then evaluated in type 1 diabetic mice. In the complex-treated group, the initial BG level was 374.2 ± 75.3 mg dl^{-1} (Fig. 2a). Mice were anaesthetized and subcutaneously injected with the complex. The BG level increased rapidly to 440.4 ± 64.0 mg dl^{-1} at 0 min because of the stress response and then gradually decreased to 137.2 ± 22.5 mg dl^{-1} within 1 h. Mean BG was maintained below 200 mg dl^{-1} for more than one week. Specifically, BG was 196.6 ± 85.4 and 245.8 ± 99.0 mg dl^{-1} at 166 and 176 h, respectively. This anti-hyperglycaemic effect and the duration of normoglycaemia were much longer than those observed with a single injection of insulin glargine (Fig. 2b,c). Impressively, BG gradually decreased again, reached 192.2 ± 21.3 mg dl^{-1} at 430 h posttreatment and remained at 242.4 ± 80.5 mg dl^{-1} at 622 h posttreatment. In comparison, mice receiving one or seven injections of insulin glargine did not have similar BG control (Fig. 2b and Supplementary Fig. 7a). BG lower than 50 mg dl^{-1} is generally defined as severe hypoglycaemia. During the whole study, BG lower than 50 mg dl^{-1} was observed for only one mouse 24 h posttreatment. The BG of diabetic mice without treatment did not self-correct (Supplementary Fig. 7b).

The BG control and GRI release behaviour of the complex were further evaluated via an intraperitoneal glucose tolerance test. Glucose was injected at a dosage of 1.5 g kg^{-1} at 15 h, 48 h, 6 days, 12 days and 21 days after complex administration (Fig. 2d–g and Supplementary Fig. 7c). Fifteen hours posttreatment, the BG of treated diabetic mice was 123.0 ± 22.6 mg dl^{-1}. Glucose administration induced a BG peak at 274.4 ± 50.0 mg dl^{-1} within 10 min, after which BG rapidly decreased to the initial level within 30 min (Fig. 2d). Of note, BG levels did not return to the initial normoglycaemic level within 120 min in healthy mice that received the glucose injection. Thus, the complex-treated mice showed enhanced BG regulation ability compared with healthy mice (Fig. 2h). Forty-eight hours posttreatment, BG levels increased to 295.2 ± 21.6 mg dl^{-1} at 10 min and returned to the initial BG level within 30 min (Fig. 2e). Six days posttreatment, initial BG levels were 124.2 ± 22.4 mg dl^{-1}, which gradually increased to 412.0 ± 99.7 mg dl^{-1} within 20 min and further gradually decreased to 164.6 ± 42.7 mg dl^{-1} within 50 min (Fig. 2f). Twelve days posttreatment, the initial BG levels were 214.8 ± 20.7 mg dl^{-1}, indicating a reduced rate of insulin release from the subcutaneous depot. After glucose administration, the BG increased sharply to 500 mg dl^{-1} in 10 min and then gradually decreased to 243.2 ± 63.3 mg dl^{-1} at 120 min (Fig. 2g). Twenty-one days after treatment, the complex did not regulate BG to its initial levels within 120 min (Supplementary Fig. 7c). As a control, insulin glargine-treated mice, similar to untreated diabetic mice, cannot regulate BG back to normal even at 6 and 15 h posttreatment (Fig. 2i,j and Supplementary Fig. 7d).

In vivo BG-triggered insulin release was further evaluated via intraperitoneal glucose administration in diabetic mice. Three days after administration of the complex (20 mg kg^{-1}), glucose was injected intraperitoneally (3 g kg^{-1}) to induce a clear BG spike (Fig. 2k). BG levels peaked at 412.0 ± 63.2 mg dl^{-1} at 15 min and decreased to 98.2 ± 29.9 mg dl^{-1} at 120 min. The insulin level increased from 65.0 ± 13.8 μU ml^{-1} to 178.9 ± 86.4 μU ml^{-1} 30 min after the glucose injection. Plasma insulin levels decreased to 97.6 ± 39.8 and 87.6 ± 21.8 μU ml^{-1} at 60 and 120 min along with the decrease in BG.

The long-term BG control capacity of the complex when administered via multiple injections was also studied in diabetic mice (Fig. 2l). The black arrows represent three injections of the complex (20, 14 and 14 mg kg^{-1} in turn). An injection was given every 168 h. The initial BG was 383.8 ± 64.2 mg dl^{-1} and the BG was controlled below 200 mg dl^{-1} for at least 22 days (164.4 ± 38.7 mg dl^{-1}). No obvious hypoglycaemia was observed during the period.

The efficacy of the insulin complex was further evaluated in three type 1 diabetic minipigs (designated Pig 1, Pig 2 and Pig 3). BG levels were monitored by a continuous glucose-monitoring system (CGMS; FreeStyle Libre, Abbott), which is accurate over the range 39.6–500.4 mg dl^{-1}. The BG measured by CGMS was consistent with that measured using a glucometer (ACCU-CHEK, Aviva). The FreeStyle Libre sensor was inserted in the legs of the minipigs. The minipigs were fed twice every day. The BG of a healthy minipig ranges between 39.6 and 100 mg dl^{-1} (Supplementary Fig. 8). Without treatment, the BG of all the diabetic minipigs remained elevated >200 mg dl^{-1}, although each minipig showed distinct glucose levels and variability (Fig. 3a). Insulin glargine (Lantus, U-100), used as a positive control, was given at 0.4, 0.6 and 0.6 U kg^{-1} for Pig 1, Pig 2 and Pig 3, respectively. Insulin glargine regulated BG for no longer than 24 h (Fig. 3b), and seven daily injections of insulin glargine can control BG in a pulsatile manner (Fig. 3c). The minipigs were treated with insulin complexes at a dose of 0.2 mg kg^{-1} for Pig 1 and 0.3 mg kg^{-1} for Pig 2 and Pig 3. The complex regulated BG levels below 200 mg dl^{-1}, with minimal BG below 40 mg dl^{-1} (Fig. 3d and Supplementary Fig. 9). Insulin complex could constantly maintain BG levels below 200 mg dl^{-1} in Pig 1 (Fig. 3d and Supplementary Fig. 9a). Insulin complex-treated Pig 2 and Pig 3 showed a gradual increase in BG but this returned to <200 mg dl^{-1} even at 120 h and 80 h posttreatment, respectively (Fig. 3d). In addition, after 168 and 144 h, the BG of Pig 2 and Pig 3 did not return to the initial BG level of >350 mg dl^{-1} (Supplementary Fig. 9b), indicating an ability to sustainably control BG for longer than 168 h. Collectively, insulin complex showed enhanced BG control compared with a single injection of insulin glargine (Extended Data Fig. 2a) and similar treatment efficacy to seven daily injections of insulin glargine with a reduced hypoglycaemia index (Extended Data Fig. 2b). In addition, serum insulin gradually decreased over time, and was still observed 7 days posttreatment (Fig. 3e). Because minipigs are physiologically more similar to humans, the ultra-long-acting performance of the complex in minipigs indicates the potential for long-acting performance in humans. Furthermore, in vivo BG-triggered insulin release was observed in the three minipigs (Fig. 3f).

The toxicity of the injected complex was evaluated in mice. Cy5-labelled PLL-FPBA was injected subcutaneously. The complex remained under the skin for more than three months (Fig. 4a), much longer than reported previously[46], probably because of the high dose

https://doi.org/10.1038/s41551-023-01138-7

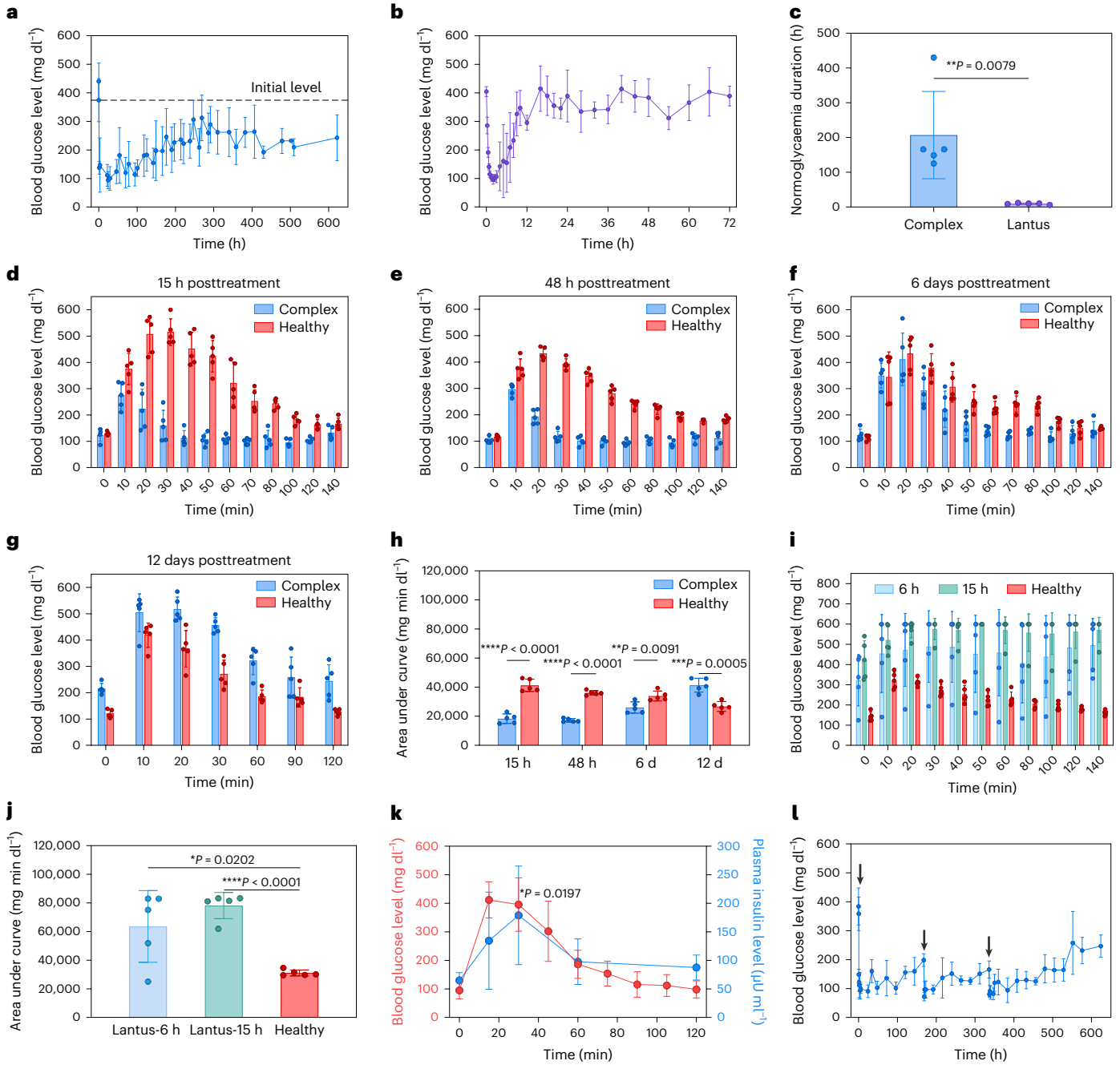

Fig. 2 | Insulin complex efficacy in type 1 diabetic mice. a, BG of diabetic mice treated with subcutaneously injected complex (20 mg kg^{-1}). Data points are means ± s.d. ($n = 5$). **b**, BG of diabetic mice treated with subcutaneously injected insulin glargine (Lantus, U-100, 40 U kg^{-1}). Data points are means ± s.d. ($n = 5$). **c**, Comparison of the duration of normoglycaemia for mice treated with complex and insulin glargine as shown in **a** and **b**. Because BG fluctuated all the time, the duration of normoglycaemia was identified as the time points when the BG is >200 mg dl^{-1} for the third time to ensure a hyperglycaemic state. Data points are means ± s.d. ($n = 5$). Two-tailed Student's *t*-test was used for statistical analysis. **d**–**g**, Intraperitoneal glucose tolerance tests. Glucose was intraperitoneally injected (1.5 g kg^{-1}) after diabetic mice had received treatment with complexes for 15 h (**d**), 48 h (**e**), 6 days (**f**) and 12 days (**g**). The insulin-equivalent dose of the complex was 20 mg kg^{-1}. Data points are means ± s.d. ($n = 5$). **h**, Area under curve statistics for **d**–**g**. Data points are means ± s.d. ($n = 5$). Two-tailed Student's *t*-test was used for statistical analysis. **i**, Intraperitoneal glucose tolerance tests. Glucose was injected intraperitoneally (1.5 g kg^{-1}) after diabetic mice had received treatment with insulin glargine (40 U kg^{-1}) for 6 and 15 h. Data points are means ± s.d. ($n = 5$). **j**, Area under curve statistics of **i**. Data points are means ± s.d. ($n = 5$). Two-tailed Student's *t*-test was used for statistical analysis. **k**, BG-triggered insulin release by intraperitoneal glucose injection (3 g kg^{-1}) at 3 days after treatment of the complex at a dose of 20 mg kg^{-1}. Data points are means ± s.d. ($n = 5$). Plasma insulin levels at various time points were compared with that at 0 h. The *P* value was calculated using one-way ANOVA with Tukey's post hoc test. **l**, BG of diabetic mice treated three times with subcutaneously injected complex. The black arrows represent three injections of the complex. The first dose of the complex was 20 mg kg^{-1}; the second and third doses were 14 mg kg^{-1}. Data points are means ± s.d. ($n = 5$).

used in this study. PLL-FPBA was mainly cleared by the liver (Fig. 4b). Laboratory markers including alkaline phosphatase, aspartate transaminase, alanine transaminase, blood urea nitrogen and creatine levels did not change with complex administration, compared with healthy mice, indicating the minimal toxicity of PLL-FPBA to the liver and kidney (Fig. 4c). Haematoxylin and eosin (H&E) and Masson's trichrome

https://doi.org/10.1038/s41551-023-01138-7

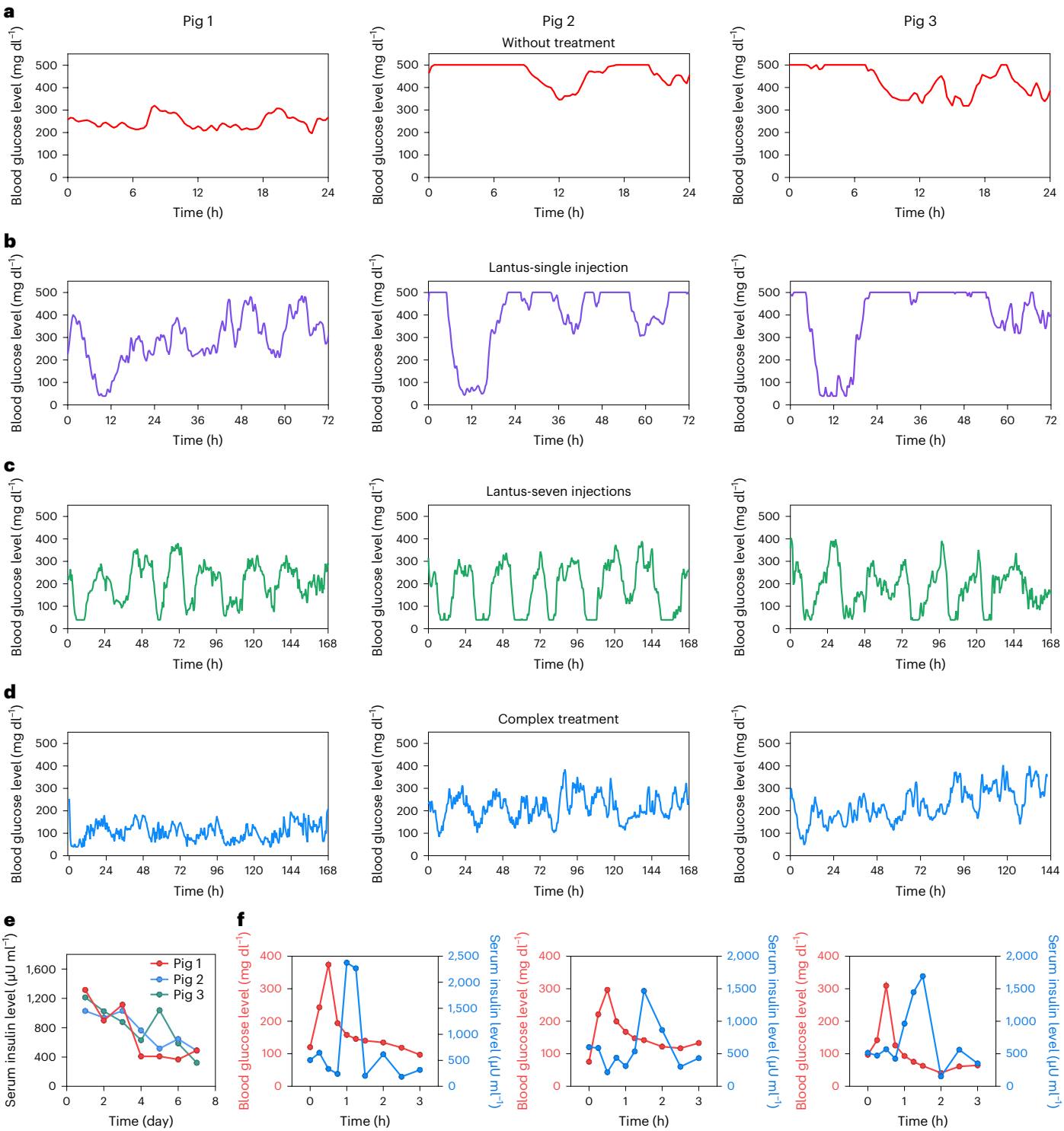

Fig. 3 | Evaluation of insulin complex in type 1 diabetic minipigs. **a**, Representative BG of type 1 diabetic minipigs without treatment. **b**, BG of type 1 diabetic minipigs treated with subcutaneously injected insulin glargine at a dose of 0.4, 0.6 and 0.6 U kg^{-1} to Pig 1, Pig 2 and Pig 3, respectively. **c**, BG of type 1 diabetic minipigs treated with seven daily injections of insulin glargine. **d**, BG of type 1 diabetic minipigs treated with one injection of insulin complex (0.2, 0.3 and 0.3 mg kg^{-1} for Pig 1, Pig 2 and Pig 3, respectively). **e**, Pharmacokinetics of insulin after a single injection of insulin complex. **f**, BG-triggered insulin release. Dextrose (5 wt%) solution was infused at a dose of 0.75 g kg^{-1} at a rate of 1 l h^{-1}, while the minipigs were kept anaesthetized using isoflurane. BG was measured using a glucose meter. Each figure is associated with data collected from one minipig.

staining were performed to evaluate the host immune response to the injected complex. Negligible neutrophil infiltration and no apparent fibrous capsule were observed at the site of the complex under the skin even at four weeks posttreatment (Fig. 4d).

This fibrous capsule-resistant capability of PLL-FPBA was further evaluated in healthy mice. Polycaprolactone (PCL) particles and silicone plates were used as positive controls[47–49]. In addition, benzoic acid-modified PLL (PLL-BA) with 64% graft degree was used to evaluate

https://doi.org/10.1038/s41551-023-01138-7

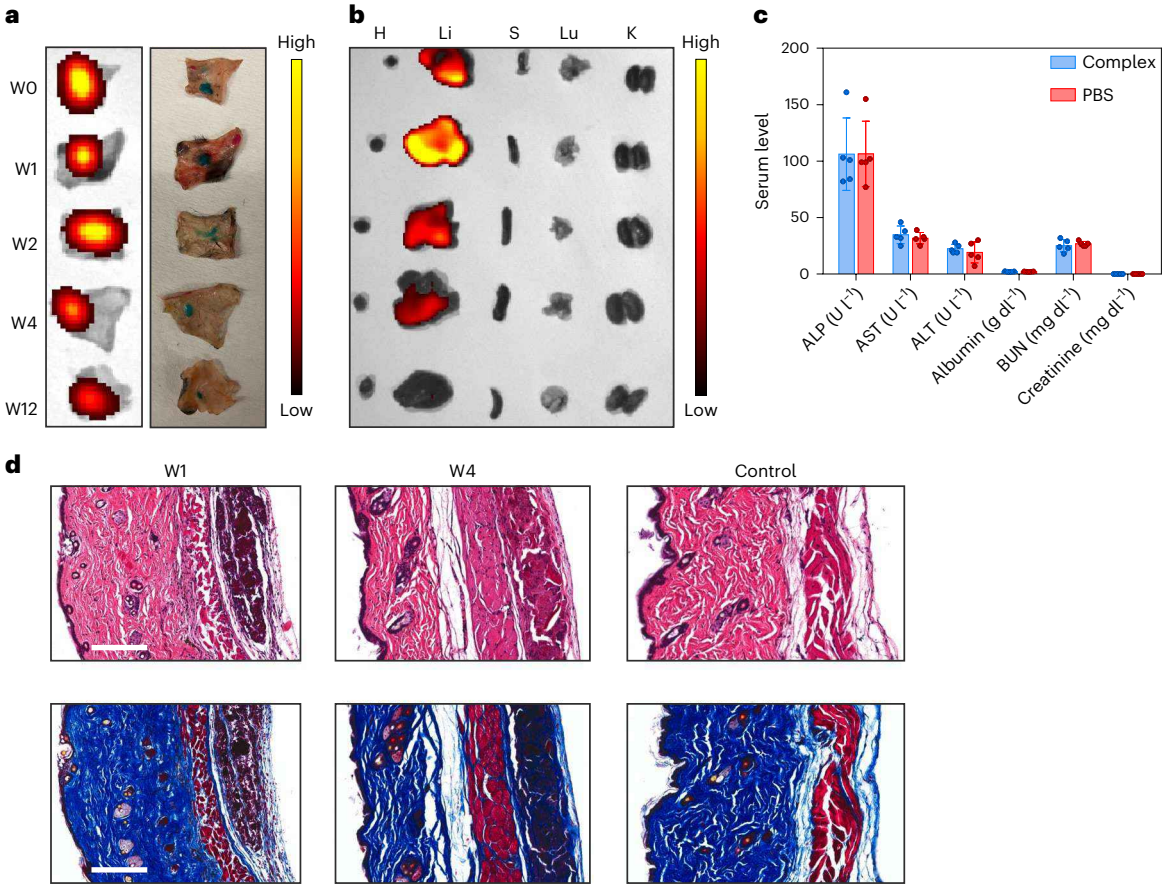

Fig. 4 | Biocompatibility study of the complex in type 1 diabetic mice. **a**, Representative fluorescence images of Cy5-labelled PLL-FPBA retained under the skin after subcutaneous injection. **b**, Biodistribution of PLL-FPBA in major organs, including heart (H), liver (Li), spleen (S), lung (Lu) and kidney (K). Samples of skin with the injected complexes and the main organs were obtained at week 0 (W0), week 1 (W1), week 2 (W2), week 4 (W4) and week 12 (W12) posttreatment. **c**, Serum levels of major biochemical parameters in diabetic mice with subcutaneously injected complex. ALP, alkaline phosphatase; ALT, alanine transaminase; AST, aspartate transaminase; BUN, blood urea nitrogen. Whole blood was obtained 1 week after treatment. Data points are means ± s.d. ($n = 5$). **d**, Representative images of skin at the injection site after H&E and Masson's trichrome staining. Skin samples from the treated sites were obtained 1 and 4 weeks posttreatment. Scale bars, 200 μm.

the effect of PBA (Supplementary Fig. 10). Two doses of PLL-FPBA (1.0 and 0.5 mg per mouse) were injected subcutaneously. These implants had similar sizes under the skin at two weeks posttreatment (Supplementary Fig. 11). Two, four and twelve weeks after subcutaneous injection, no obvious fibrous capsules were identified surrounding PLL-FPBA (Supplementary Figs. 11–13). As a comparison, the PCL particles and silicone plates triggered thick and dense collagen fibre layer surrounding the implants. Two and four weeks after implantation, a thick immune cell layer was identified at the surface of the PCL particles and silicone plates. By contrast, negligible immune cell accumulation was found around the PLL-FPBA and PLL-BA implants. F4/80, a macrophage marker, was stained red by immunofluorescence. A reduced density of red fluorescence around the PLL-FPBA implant could be observed compared with that surrounding PCL particles and silicone plates (Fig. 5a). The cytokine levels surrounding the implants were also evaluated (Fig. 5b,c). PCL implants induced the most severe accumulation of tumour necrosis factor (TNFα), interleukin-6 (IL-6), IL-10, IL-12 and IL-17 surrounding the implants; silicone plates also triggered obvious accumulations. By contrast, low levels of all cytokines were identified in the space surrounding both PLL-FPBA and PLL-BA, indicating a minor role for FPBA in reducing the host immune response. Of note, the size of the PLL-FPBA and PLL-BA implants decreased gradually over time because of the inherent biodegradability of the PLL backbone (Supplementary Figs. 11–13). The slow removal of PLL-FPBA led to a weak adherence of collagen fibre on the surface of the implants, resulting in the resistance to fibrous capsule formation. In addition, α-smooth muscle actin (α-SMA) was identified surrounding the silicone plate and PLL-FPBA implants, indicating their potential for stimulating angiogenesis (Fig. 5a).

Discussion

We have reported the development of a GRI formulation that can dynamically regulate BG within a normal range with minimal hypoglycaemia risk for a prolonged period following administration. The complex had ultra-low free-insulin concentrations of 20 μg ml^{-1} under normoglycaemic conditions because of the tight and glucose-responsive electrostatic attraction and PBA–diol complexation. Thus, the complex could be safely injected at a dose as high as 20 mg kg^{-1}. In type 1 diabetic mice, this complex dynamically regulated BG below 200 mg dl^{-1} for longer than one week and exhibited anti-hyperglycaemic effects for longer than three weeks. Upon intraperitoneal glucose administration, the complex corrected BG to normal levels within 2 h, even 12 days after the complex injection. Notably, the BG spike after the glucose challenge was accompanied by an insulin spike, indicating that the BG spike triggered insulin release from the complex depot. The complex also showed the ability to normalize BG for longer than 120 h in type 1 diabetic minipigs. The long performance of the complex in both mice and minipigs is probably because of the complex's ultra-low free-insulin

https://doi.org/10.1038/s41551-023-01138-7

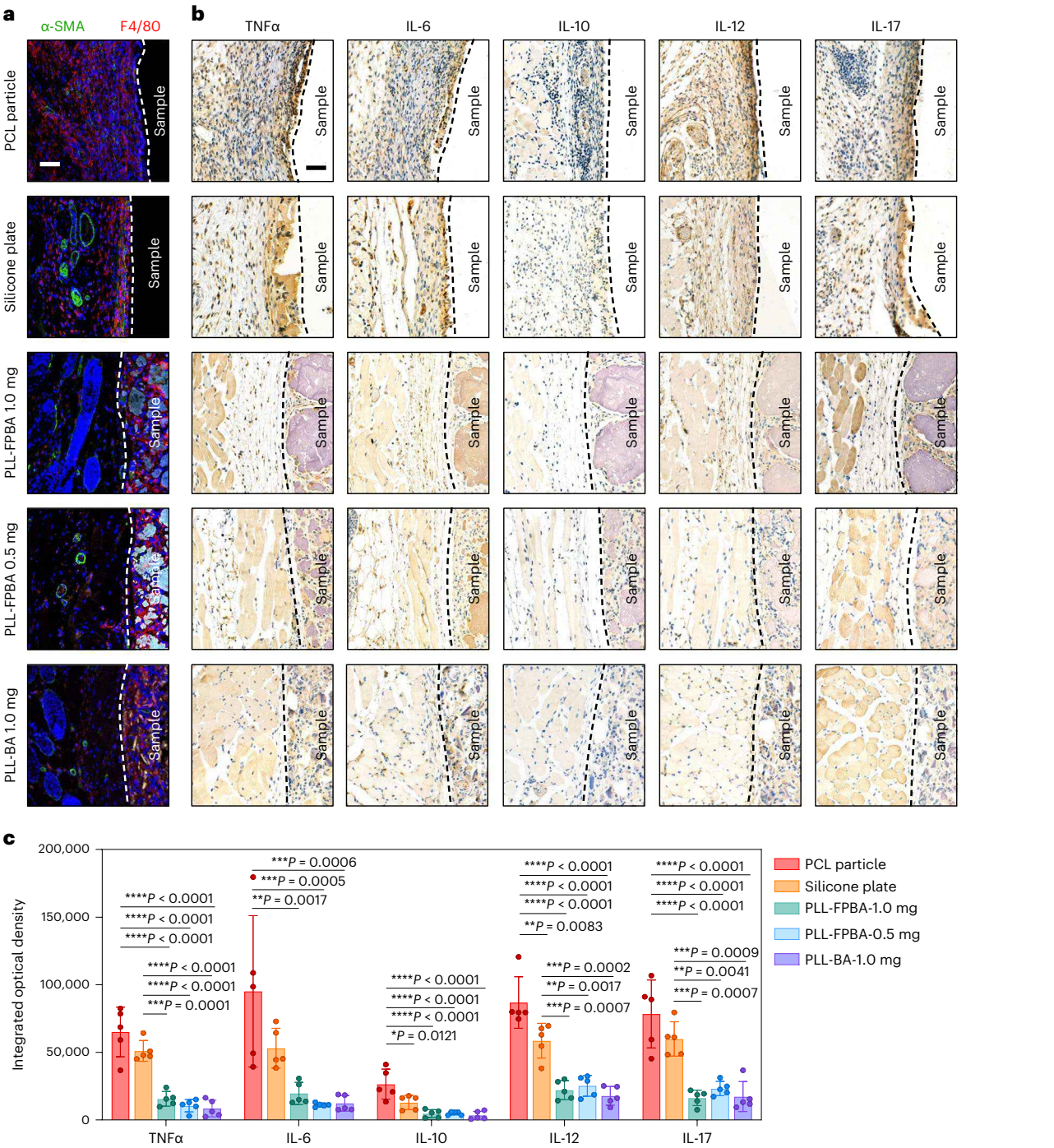

Fig. 5 | Immunofluorescence and immunohistochemical staining of the skin at the site of implants after 2 weeks. a, Immunofluorescence staining of macrophage biomarker (F4/80, red) and α-SMA (green). Nuclei were stained in blue. Scale bars, 50 μm. **b**, Immunohistochemical staining of TNFα, IL-6, IL-10, IL-12 and IL-17. Scale bars, 50 μm. **c**, The integrated optical density within 100 μm around the implants. Data points are means ± s.d. ($n = 5$). The cytokine level of each group was compared with the others. One-way ANOVA with Tukey's post hoc tests was used for multiple comparisons. $P \geq 0.05$ is not shown.

level and resistance to fibrous capsule formation. In both mouse and minipig studies, negligible hypoglycaemia was observed during treatment. Moreover, PLL-FPBA was gradually eliminated from the injection depot and showed negligible toxicity to the liver and kidney, together with almost absent fibrous capsule formation under the skin. In the long term, a balance is assumed to be established between the amount of injected PLL-FPBA and cleared PLL-FPBA. Thus, the long-term toxicity of the complex formulation needs to be thoroughly evaluated for clinical translation.

Methods

Materials

The 4-Carboxy-3-fluorophenylboronic acid was purchased from Aladdin. All other chemicals were purchased from Sigma-Aldrich. Recombinant human insulin was purchased from Thermo Fisher Scientific (catalogue no. A113811IJ). PLL with a molecular weight of 30–70 kg mol^{-1} was obtained from Sigma and used directly for FPBA modification. The materials were used as received. PLL-FPBA, PLL-BA and Glu-insulin were synthesized using the reported methods and were characterized before

use. The silicone plate was made by mixing prepolymer (Sylgard 184, DOWSIL) at a ratio of 10:1, degassing and then pouring it into plastic dishes to give a plate thickness of ~1 mm. The layer was cured at 80 °C for 2 h and divided into round plates with a diameter of ~5 mm.

Preparation of insulin complex

Glu-insulin (1 mg) and PLL-FPBA (1 mg) dissolved in acidified water (0.1 ml) were mixed and NaOH aqueous solution (1 M) was added to adjust the pH to 7.4, inducing formation of a white precipitate. The supernatant was removed after centrifugation, followed by the addition of PBS (10 mM, pH 7.4, 1 ml). Unencapsulated insulin in the supernatant was measured using the Bradford reagent. The insulin loading efficiency (LE) is defined as LE = A/C, where A is the amount of insulin loaded in the complex and C is the amount of insulin used.

Characterization of Glu-insulin

An Easy-nLC 1200 system coupled with a Q Exactive Hybrid Quadrupole-Orbitrap Mass Spectrometer (Thermo Fisher Scientific) with an electrospray ionization nanospray source was used. To confirm the modification site, Glu-insulin was completely reduced by DL-dithiothreitol and iodoacetamide solution was added to give a final concentration of 50 mmol l^{-1}. The mixture was reacted in the dark for 40 min. The solvent was desalted using a self-filled desalting column and evaporated. A species at ~1,395 m/z that possibly corresponded to the singly modified α chain was observed. The peptide was collected for tandem mass spectrometry. The raw mass spectrometry files were analysed and searched against the target protein database based on the species of the samples using Byonic. The result supported the conclusion that the modification site of gluconic acid is the N-terminal of the insulin α chain (A1).

Preparation and characterization of fluorescence dye-labelled Glu-insulin and PLL-FPBA

FITC (7.2 mg) dissolved in dimethylsulfoxide (3 ml) was added to Glu-insulin (100 mg) dissolved in $NaHCO_3$ (0.1 M, 5 ml). The mixture was stirred at room temperature overnight and dialysed in deionized water (3× 4 l). FITC-labelled insulin was obtained after lyophilization. Cy5-labelled PLL-FPBA was synthesized using a similar procedure. The complex prepared from FITC-labelled Glu-insulin and Cy5-labelled PLL-FPBA was observed using a fluorescence microscope (T1, Nikon).

TEM and SEM characterization of Glu-insulin complex

Insulin complex (insulin-equivalent concentration of 1 mg ml^{-1}) was dispersed and suspended in water (1 ml), diluted tenfold and dropped onto a copper mesh. Uranyl acetate solution (5%, 10 µl) was added to the copper mesh and left for 10 min. A filtrate paper was used to remove the solution and the sample was observed using TEM (Talos L120C, Thermo Fisher Scientific). The same sample was also dropped onto a silicon wafer, dried naturally and observed using SEM (Nova Nano 450, Thermo Fisher Scientific).

GRI release at various glucose solutions

Insulin complexes were resuspended in PBS at pH 7.4. The final total Glu-insulin equivalent concentration was set to 1 mg ml^{-1}. The Glu-insulin concentration in the supernatant before the addition of glucose was measured immediately and set as 0 µg ml^{-1}. Concentrated glucose solution (300 mg ml^{-1}) was then added to complex suspensions in Eppendorf tubes (1 ml per tube, $n = 3$) to obtain glucose solutions of 0, 100, 200 and 400 mg dl^{-1}. The suspensions were incubated at 37 °C. Suspension samples (30 µl) were collected after vigorous shaking at predetermined time points (0.2, 1, 2 and 5 h incubation). The obtained samples were centrifuged at 40,000g for 5 min. The supernatant (10 µl) was collected to measure the Glu-insulin concentration using Bradford assay reagent. The concentration of Glu-insulin was calibrated according to a standard curve.

Glucose-responsive pulsatile and cumulative insulin release

The insulin complex was exposed to glucose solutions with concentrations of 100 and 400 mg dl^{-1} in cycles ($n = 3$). To begin the experiment, the insulin complex (equivalent to 1 mg of insulin) was centrifuged and then mixed with 1 ml of a 400 mg dl^{-1} glucose solution. After 10 min, the suspension was centrifuged again and the supernatant was collected to determine the insulin concentration before addition of 1 ml of a 100 mg dl^{-1} glucose solution. After 10 min, the suspension was centrifuged again and the supernatant was collected to identify the concentration of insulin before addition of 1 ml of a 400 mg dl^{-1} glucose solution. This process was repeated three times. The insulin concentration of the supernatant was determined using the Bradford reagent and calibrated using a standard curve. In the same way, cumulative insulin release from complex was tested. Complexes (equivalent to 1 mg of insulin) were exposed to 1 ml of glucose solution containing 0, 100, 200 and 400 mg dl^{-1} glucose ($n = 5$). The complexes were incubated in each solution for 10 min.

Western blotting to evaluate the activity of Glu-insulin

The HepG2 cell line was obtained from the National Collection of Authenticated Cell Cultures (Shanghai, China). HepG2 cells were cultured in DMEM with 10% FBS and 1% penicillin/streptomycin. Cells were serum-starved for 12 h after the culture reached 80–90% confluence. The cells were then washed and exposed to medium containing insulin or Glu-insulin (0, 0.1, 1, 5, 10, 50, 100 nM) for 10 min ($n = 3$). Cell lysates were prepared by lysing cells in ice-cold RIPA buffer (Beyotime) containing protease and phosphatase inhibitors (Meilunbio). Lysate was cleared by centrifugation at 16,000g for 10 min at 4 °C. The protein concentration was determined using a BCA assay (Beyotime) and samples were boiled in 1× Laemmli loading buffer (Bio-Rad) containing 2.5% β-mercaptoethanol. Proteins were separated by 10% SDS–PAGE gels and transferred to 0.45 µm polyvinylidene difluoride membranes (Sigma-Aldrich). Membranes were blocked with 5% non-fat milk in phosphate-buffered saline with 0.1% Tween-20 and probed using target-specific antibodies (anti-phospho-Akt (Cell Signaling Technology, catalogue no. 4060, 1:2,000), anti-Akt (Cell Signaling Technology, catalogue no. 4691, 1:1,000) and anti-β-actin (Diagbio, catalogue no. db7283, 1:1,000)) in primary antibody dilution buffer (Beyotime). Bound antibodies were detected using horseradish peroxidase-conjugated secondary antibodies (Hangzhou Fude, catalogue no. FDR007, 1:10,000) and ECL Western Blotting Substrate (Thermo Fisher Scientific), according to the manufacturer's instructions.

Type 1 diabetes treatment study in mice

All animal procedures were performed following the Guidelines for Care and Use of Laboratory Animals of Zhejiang University (protocol no. ZJU20220299). C57BL/6 mice (aged 6–8 weeks) were purchased from Hangzhou Medical College. Type 1 diabetic mice were induced by injecting STZ at a dose of 150 mg kg^{-1}. The diabetic mice were maintained with a standard diet in 12:12 h light/dark cycles, allowing free access to food and water during the experiment. The ambient temperature was 20–26 °C and the relative humidity was 50–70%. Diabetic mice were grouped ($n = 5$) and received a subcutaneous injection of insulin glargine (40 U kg^{-1}) and insulin complex (2.5, 5, 10 and 20 mg kg^{-1}). For multiple injections, the insulin complex was injected every 168 h ($n = 5$). The insulin-equivalent dose of the second and third injections was reduced to 14 mg kg^{-1}. As a control, insulin glargine at a dose of 40 U kg^{-1} was injected every 24 h for seven consecutive days and stopped for one day. In addition, the BG of diabetic mice without treatment was continuously monitored for one month. BG was measured using a glucose meter (Aviva, ACCU-CHEK).

Intraperitoneal glucose tolerance test

Diabetic mice receiving complex treatment ($n = 5$) were subjected to intraperitoneal glucose administration (1.5 g kg^{-1}) at various time

points posttreatment. Time points of 15 h, 48 h, 6 days, 12 days and 21 days were selected for intraperitoneal glucose tolerance test to evaluate the BG regulation capability of insulin complex in the short and long term. Healthy mice ($n = 5$) and diabetic mice treated with insulin glargine ($n = 5$) were used as the control groups. Area under the curve was calculated using Originlab 2018 software. Blood samples (40 µl) were collected for BG measurement and plasma extraction. Plasma insulin levels were measured using a human insulin ELISA kit (Invitrogen).

Type 1 diabetes treatment in STZ-induced diabetic minipigs

Six-month-old Bama miniature pigs were intravenously injected with STZ (150 mg kg^{-1}) to induce the type 1 diabetes. The BG of minipigs was stabilized, and diabetic minipigs were used in the study after one month. The minipigs were fed twice a day, either with or without treatment. BG was monitored by CGMS (FreeStyle Libre, Abbott). Insulin glargine (Lantus, Sanofi) was used once a day for usual BG control. The administration of insulin glargine was paused for 48 h before evaluating the efficacy of therapeutic BG control. The three minipigs received a subcutaneous injection of insulin glargine at a dose of 0.4, 0.6 or 0.6 U kg^{-1}, respectively and were treated with subcutaneously injected complex at a dose of 0.2, 0.3 and 0.3 mg kg^{-1} in turn.

In vivo evaluation of glucose-triggered insulin release in minipigs

Three diabetic minipigs were treated subcutaneously with insulin complex at a dose of 0.2, 0.3 and 0.3 mg kg^{-1} for Pig 1, Pig 2 and Pig 3, respectively. Eight hours later, dextrose (5 wt%) solution was infused at a dose of 0.75 g kg^{-1} at a rate of 1 l h^{-1}, while the minipigs were kept anaesthetized using isoflurane. Blood was collected from the external jugular vein before and during the experiment at predetermined intervals. Blood (2 ml) was placed in serum-collecting tubes (BD Vacutainer) and serum was collected following the protocol. Serum insulin levels were measured by human insulin ELISA kit (Elabscience).

Toxicity evaluation in diabetic mice

Diabetic mice were injected subcutaneously with insulin complex at an insulin-equivalent dose of 20 mg kg^{-1} or with PBS ($n = 5$). After one week, the blood was collected for analysing alkaline phosphatase, aspartate transaminase, alanine transaminase, albumin, blood urea nitrogen and creatinine levels in serum to evaluate the toxicity to the liver and kidney. In addition, PLL-FPBA was labelled with sulfo-Cy5 and the presence of a PLL-FPBA depot was monitored with living imaging (IVIS Lumina III, PerkinElmer).

Host response evaluation of PLL-FPBA in mice

C57BL/6 mice (aged 6–8 weeks) were purchased from Hangzhou Medical College. Mice were implanted with a PCL particle (diameter, 5 mm; number-average molecular weight of 45,000 g mol^{-1}, Sigma), silicone plate (diameter, 5 mm), PLL-FPBA (0.5 mg, 1.0 mg) and PLL-BA (1.0 mg). All materials were sterilized. Surgery was performed under isoflurane anaesthesia and aseptic conditions. Skin samples were disinfected before and after surgery. Approximately 8 mm longitudinal incisions were made on the back of the mice for implantation of the PCL particles and silicone plates. The incision was sufficiently distant from the implantation site to avoid the effects of the wound. The skin was sutured after the materials were implanted. PLL-FPBA or PLL-BA suspended in 0.1 ml of PBS was injected subcutaneously. Five replicates for each type of material were implanted into mice. After 2, 4 and 12 weeks, the mice were euthanized, and the skin with the implants was removed, fixed in 4% paraformaldehyde for more than 24 h and embedded in paraffin. Untreated mice from the same batch were used as a blank control. Each skin tissue sample was sectioned at a thickness of 3–4 µm for H&E and Masson's trichrome staining. Immunofluorescence staining of α-SMA (Abcam, catalogue no. ab240654, 1:50,000; Alexa Fluor 488 conjugate, Cell Signaling Technology, catalogue no. 4412, 1:1,000), F4/80 (Abcam, catalogue no. ab300421, 1:5,000; Alexa Fluor 594 conjugate, Cell Signaling Technology, catalogue no. 8890, 1:1,000) and immunohistochemical staining of TNFα (Immunoway, catalogue no. YT4689, 1:200), IL-6 (Affinity Biosciences, catalogue no. DF6087, 1:100), IL-10 (Affinity Biosciences, catalogue no. DF6894, 1:100), IL-12 (Affinity Biosciences, catalogue no. AF5133, 1:100) and IL-17 (Affinity Biosciences, catalogue no. DF6127, 1:100) were also performed. Immunofluorescence images were recorded on a laser scanning confocal microscope (ECLIPSE Ti2, Nikon) and analysed using NIS-Elements Viewer (v.5.21). The H&E, Masson's trichrome and immunohistochemistry images were collected by digital slice scanner (VS200, Olympus) and analysed using Olympus Image Viewer. The positive staining analysis of immunohistochemical images was performed on ImageJ2 (Fiji) (within 100 µm of the implant–tissue interface).

Statistical analysis

One-way analysis of variance (ANOVA) with Tukey's post hoc tests was used for multiple comparisons. Unpaired Student's *t*-test was used to analyse the difference between two groups.

Reporting summary

Further information on research design is available in the Nature Portfolio Reporting Summary linked to this article.

Data availability

The authors declare that all of the data supporting the findings of this study are available within the paper and its Supplementary Information. Source data are provided with this paper.

References

1. Sun, H. et al. IDF diabetes atlas: global, regional and country-level diabetes prevalence estimates for 2021 and projections for 2045. *Diabetes Res. Clin. Pract.* **183**, 109119 (2022).
2. Garg, S. K., Rewers, A. H. & Akturk, H. K. Ever-increasing insulin-requiring patients globally. *Diabetes Technol. Ther.* **20**, S21–S24 (2018).
3. Cefalu, W. T. et al. Insulin access and affordability working group: conclusions and recommendations. *Diabetes Care* **41**, 1299–1311 (2018).
4. Katsarou, A. et al. Type 1 diabetes mellitus. *Nat. Rev. Dis. Primers* **3**, 17016 (2017).
5. McCall, A. L. Insulin therapy and hypoglycemia. *Endocrinol. Metab. Clin. North Am.* **41**, 57–87 (2012).
6. Gordijo, C. R. et al. Nanotechnology-enabled closed loop insulin delivery device: in vitro and in vivo evaluation of glucose-regulated insulin release for diabetes control. *Adv. Funct. Mater.* **21**, 73–82 (2011).
7. Veiseh, O., Tang, B., Whitehead, K. A., Anderson, D. G. & Langer, R. Managing diabetes with nanomedicine: challenges and opportunities. *Nat. Rev. Drug Discov.* **14**, 45–57 (2015).
8. Lu, Y., Aimetti, A. A., Langer, R. & Gu, Z. Bioresponsive materials.*Nat. Rev. Mater.* **2**, 16075 (2017).
9. Bakh, N. A. et al. Glucose-responsive insulin by molecular and physical design. *Nat. Chem.* **9**, 937–943 (2017).
10. Wang, J. et al. Glucose-responsive insulin and delivery systems: innovation and translation. *Adv. Mater.* **32**, e1902004 (2020).
11. Jarosinski, M. A., Dhayalan, B., Rege, N., Chatterjee, D. & Weiss, M. A. 'Smart' insulin-delivery technologies and intrinsic glucose-responsive insulin analogues. *Diabetologia* **64**, 1016–1029 (2021).
12. Wang, Z. J., Wang, J. Q., Kahkoska, A. R., Buse, J. B. & Gu, Z. Developing insulin delivery devices with glucose responsiveness. *Trends Pharmacol. Sci.* **42**, 31–44 (2021).

13. Kitano, S., Koyama, Y., Kataoka, K., Okano, T. & Sakurai, Y. A novel drug delivery system utilizing a glucose responsive polymer complex between poly(vinyl alcohol) and poly(*N*-vinyl-2-pyrrolidone) with a phenylboronic acid moiety. *J. Control. Release* **19**, 161–170 (1992).
14. Shiino, D. et al. Amine containing phenylboronic acid gel for glucose-responsive insulin release under physiological pH. *J. Control. Release* **37**, 269–276 (1995).
15. Hisamitsu, I., Kataoka, K., Okano, T. & Sakurai, Y. Glucose-responsive gel from phenylborate polymer and poly(vinyl alcohol): prompt response at physiological pH through the interaction of borate with amino group in the gel. *Pharm. Res.* **14**, 289–293 (1997).
16. Kataoka, K., Miyazaki, H., Bunya, M., Okano, T. & Sakurai, Y. Totally synthetic polymer gels responding to external glucose concentration: their preparation and application to on–off regulation of insulin release. *J. Am. Chem. Soc.* **120**, 12694–12695 (1998).
17. Shen, D. et al. Recent progress in design and preparation of glucose-responsive insulin delivery systems. *J. Control. Release* **321**, 236–258 (2020).
18. Matsumoto, A., Yoshida, R. & Kataoka, K. Glucose-responsive polymer gel bearing phenylborate derivative as a glucose-sensing moiety operating at the physiological pH. *Biomacromolecules* **5**, 1038–1045 (2004).
19. Zhao, Y., Trewyn, B. G., Slowing, I. I. & Lin, V. S. Mesoporous silica nanoparticle-based double drug delivery system for glucose-responsive controlled release of insulin and cyclic AMP. *J. Am. Chem. Soc.* **131**, 8398–8400 (2009).
20. Liang, L. & Liu, Z. A self-assembled molecular team of boronic acids at the gold surface for specific capture of cis-diol biomolecules at neutral pH. *Chem. Commun. (Camb.)* **47**, 2255–2257 (2011).
21. Matsumoto, A. et al. A synthetic approach toward a self-regulated insulin delivery system. *Angew. Chem. Int. Ed. Engl.* **51**, 2124–2128 (2012).
22. Chou, D. H. et al. Glucose-responsive insulin activity by covalent modification with aliphatic phenylboronic acid conjugates. *Proc. Natl Acad. Sci. USA* **112**, 2401–2406 (2015).
23. Dong, Y. et al. Injectable and glucose-responsive hydrogels based on boronic acid–glucose complexation. *Langmuir* **32**, 8743–8747 (2016).
24. Brooks, W. L. A. & Sumerlin, B. S. Synthesis and applications of boronic acid-containing polymers: from materials to medicine. *Chem. Rev.* **116**, 1375–1397 (2016).
25. Matsumoto, A. et al. Synthetic 'smart gel' provides glucose-responsive insulin delivery in diabetic mice. *Sci. Adv.* **3**, eaaq0723 (2017).
26. Yu, J. C. et al. Glucose-responsive oral insulin delivery for postprandial glycemic regulation. *Nano Res.* **12**, 1539–1545 (2019).
27. Wang, J. et al. Charge-switchable polymeric complex for glucose-responsive insulin delivery in mice and pigs. *Sci. Adv.* **5**, eaaw4357 (2019).
28. Yu, J. et al. Glucose-responsive insulin patch for the regulation of blood glucose in mice and minipigs. *Nat. Biomed. Eng.* **4**, 499–506 (2020).
29. Xiao, Y., Sun, H. & Du, J. Sugar-breathing glycopolymersomes for regulating glucose level. *J. Am. Chem. Soc.* **139**, 7640–7647 (2017).
30. Wang, C. et al. Red blood cells for glucose-responsive insulin delivery. *Adv. Mater.* **29**, 1606617 (2017).
31. Yang, R. et al. A glucose-responsive insulin therapy protects animals against hypoglycemia. *JCI Insight* **3**, e97476 (2018).
32. Gu, Z. et al. Glucose-responsive microgels integrated with enzyme nanocapsules for closed-loop insulin delivery. *ACS Nano* **7**, 6758–6766 (2013).
33. Gu, Z. et al. Injectable nano-network for glucose-mediated insulin delivery. *ACS Nano* **7**, 4194–4201 (2013).
34. Yu, J. C. et al. Microneedle-array patches loaded with hypoxia-sensitive vesicles provide fast glucose-responsive insulin delivery. *Proc. Natl Acad. Sci. USA* **112**, 8260–8265 (2015).
35. Yu, J. et al. Hypoxia and H_2O_2 dual-sensitive vesicles for enhanced glucose-responsive insulin delivery. *Nano Lett.* **17**, 733–739 (2017).
36. Wang, J. et al. Core–shell microneedle gel for self-regulated insulin delivery. *ACS Nano* **12**, 2466–2473 (2018).
37. Chen, Z. et al. Synthetic beta cells for fusion-mediated dynamic insulin secretion. *Nat. Chem. Biol.* **14**, 86–93 (2018).
38. Podual, K., Doyle, F. J. & Peppas, N. A. Glucose-sensitivity of glucose oxidase-containing cationic copolymer hydrogels having poly(ethylene glycol) grafts. *J. Control. Release* **67**, 9–17 (2000).
39. Podual, K., Doyle, F. J. & Peppas, N. A. Dynamic behavior of glucose oxidase-containing microparticles of poly(ethylene glycol)-grafted cationic hydrogels in an environment of changing pH. *Biomaterials* **21**, 1439–1450 (2000).
40. Podual, K., Doyle, F. J. & Peppas, N. A. Preparation and dynamic response of cationic copolymer hydrogels containing glucose oxidase. *Polymer* **41**, 3975–3983 (2000).
41. Shiino, D. et al. Preparation and characterization of a glucose-responsive insulin-releasing polymer device. *Biomaterials* **15**, 121–128 (1994).
42. Chang, R. et al. Nanoporous immunoprotective device for stem-cell-derived beta-cell replacement therapy. *ACS Nano* **11**, 7747–7757 (2017).
43. Liu, W. et al. Macroencapsulation devices for cell therapy. *Engineering* **13**, 53–70 (2022).
44. Qiu, Y. B. et al. Long-lasting designer insulin with glucose-dependent solubility markedly reduces risk of hypoglycemia. *Adv. Ther. (Weinh)* **2**, 1900128 (2019).
45. Chinisaz, M. et al. Structure and function of anhydride-modified forms of human insulin: in silico, in vitro and in vivo studies. *Eur. J. Pharm. Sci.* **96**, 342–350 (2017).
46. Wang, J. et al. Injectable biodegradable polymeric complex for glucose-responsive insulin delivery. *ACS Nano* **15**, 4294–4304 (2021).
47. Zhang, D. et al. Dealing with the foreign-body response to implanted biomaterials: strategies and applications of new materials. *Adv. Funct. Mater.* **31**, 2007226 (2021).
48. Zhang, D. et al. Bio-inspired poly-DL-serine materials resist the foreign-body response. *Nat. Commun.* **12**, 5327 (2021).
49. Chung, L. et al. Interleukin 17 and senescent cells regulate the foreign body response to synthetic material implants in mice and humans. *Sci. Transl. Med.* **12**, eaax3799 (2020).

Acknowledgements

This work was supported by the grants from National Key R&D Program of China (grant no. 2022YFE0202200), Juvenile Diabetes Research Foundation (grant nos 2-SRA-2021-1064-M-B, 2-SRA-2022-1159-M-B), and Zhejiang University's start-up packages, the Kunpeng Program grant and Fundamental Research Funds for the Central Universities (grant no. 2021FZZX001-46). A.R.K. is supported by the National Center for Advancing Translational Sciences, National Institutes of Health, through grant no. KL2TR002490. The project was supported by grant no. UL1TR002489 from the Clinical and Translational Science Award programme of the National Center for Advancing Translational Sciences, National Institutes of Health. We appreciate the help from G. Zhu and Y. Zhang (Cryo-EM Centre, Zhejiang University) for processing of samples for electron microscopy, D. Guo (Division of Hepatobiliary and Pancreatic Surgery, Department of Surgery, The First Affiliated Hospital, Zhejiang University School of Medicine) for slicing and staining skin tissue, C. Sun (Analysis Center of Agrobiology and Environmental Sciences, Zhejiang University) for MALDI-TOF mass

analysis and D. Xu (Animal Center, Zhejiang University) for taking care of the minipigs.

Author contributions

Z.G., J.B.B. and J.W. conceived and designed the study. J.W., J.Z., X.W., W.L., Y.W., W.Z., T.S., Y.Z., Y.L., K.J. and J.X. conducted experiments and obtained data. X.Z. and P.Z. provided experimental and theoretical guidance, respectively. H.Z. and Y.X. conducted western blot experiments and provided theoretical support, respectively. J.W., J.Z., X.W., W.L., Y.Z., W.Z., T.S., J.B.B., A.R.K. and Z.G. analysed the data and wrote the paper.

Competing interests

Z.G. is the co-founder of Zenomics Inc., Zcapsule Inc. and μZen Inc. The remaining authors declare no competing interests.

Additional information

Extended data is available for this paper at https://doi.org/10.1038/s41551-023-01138-7.

Supplementary information The online version contains supplementary material available at https://doi.org/10.1038/s41551-023-01138-7.

Correspondence and requests for materials should be addressed to Jinqiang Wang or Zhen Gu.

Peer review information *Nature Biomedical Engineering* thanks the anonymous reviewer(s) for their contribution to the peer review of this work.

https://doi.org/10.1038/s41551-023-01138-7

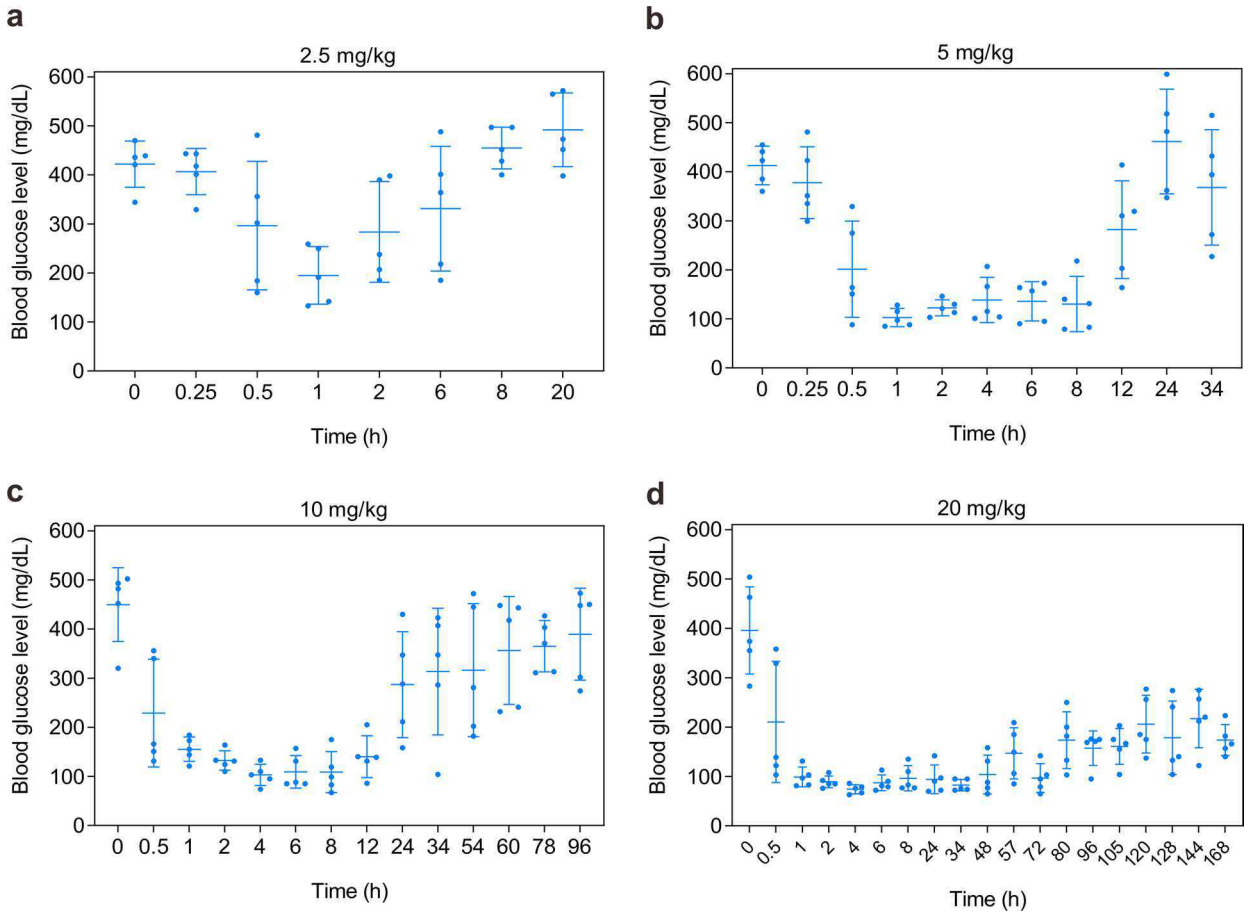

Extended Data Fig. 1 | BG regulation by the insulin complex in diabetic mice. The dose was set to 2.5 (**a**), 5 (**b**), 10 (**c**), and 20 (**d**) mg/kg. Insulin complex was subcutaneously injected. Data points are means ± SD ($n = 5$).

https://doi.org/10.1038/s41551-023-01138-7

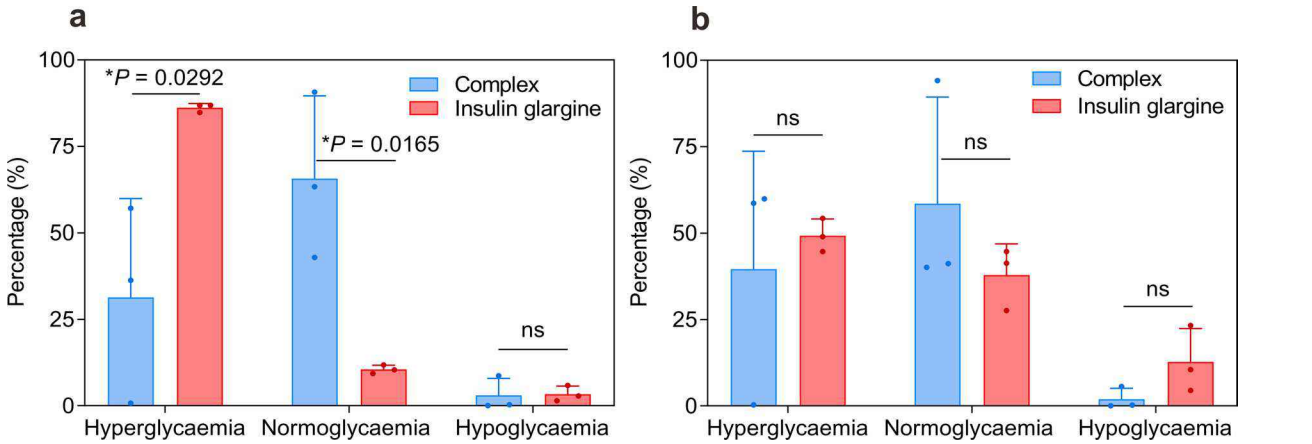

Extended Data Fig. 2 | Time proportion in the range of hyperglycaemia, normoglycaemia and hypoglycaemia in diabetic minipigs after subcutaneous injection of the complex or of insulin glargine. Hyperglycaemia, normoglycaemia, and hypoglycaemia were defined as BG more than 200 mg/dL, 50-200 mg/dL, and less than 50 mg/dL. Data points are means ± SD ($n = 3$). **a**, Both insulin glargine (0.4 to 0.6 U/kg) and complex (0.2 to 0.3 mg/kg) were injected once at the beginning of treatment. As BG was monitored for 3 days for the insulin-treated group, BG within three days was included in the statistical analysis. **b**, Insulin glargine (0.4 to 0.6 U/kg) was injected daily for 7 days, and complex (0.2 to 0.3 mg/kg) was injected once at the beginning of treatment. BG within 7 days was included in the statistical analysis. Two-tailed Student's *t*-test was used for statistical analysis.

nature portfolio

Corresponding author(s): Zhen Gu

Last updated by author(s): Sep 5, 2022

Reporting Summary

Nature Portfolio wishes to improve the reproducibility of the work that we publish. This form provides structure for consistency and transparency in reporting. For further information on Nature Portfolio policies, see our Editorial Policies and the Editorial Policy Checklist.

Statistics

For all statistical analyses, confirm that the following items are present in the figure legend, table legend, main text, or Methods section.

n/a	Confirmed
☐	☒ The exact sample size (*n*) for each experimental group/condition, given as a discrete number and unit of measurement
☐	☒ A statement on whether measurements were taken from distinct samples or whether the same sample was measured repeatedly
☐	☒ The statistical test(s) used AND whether they are one- or two-sided *Only common tests should be described solely by name; describe more complex techniques in the Methods section.*
☒	☐ A description of all covariates tested
☐	☒ A description of any assumptions or corrections, such as tests of normality and adjustment for multiple comparisons
☐	☒ A full description of the statistical parameters including central tendency (e.g. means) or other basic estimates (e.g. regression coefficient) AND variation (e.g. standard deviation) or associated estimates of uncertainty (e.g. confidence intervals)
☐	☒ For null hypothesis testing, the test statistic (e.g. *F*, *t*, *r*) with confidence intervals, effect sizes, degrees of freedom and *P* value noted *Give P values as exact values whenever suitable.*
☒	☐ For Bayesian analysis, information on the choice of priors and Markov chain Monte Carlo settings
☒	☐ For hierarchical and complex designs, identification of the appropriate level for tests and full reporting of outcomes
☒	☐ Estimates of effect sizes (e.g. Cohen's *d*, Pearson's *r*), indicating how they were calculated

Our web collection on statistics for biologists contains articles on many of the points above.

Software and code

Policy information about availability of computer code

Data collection	Nuclear magnetic resonance (NMR) spectra include 1H-NMR, 13C-NMR and B-NMR. 1H-NMR and 13C-NMR were recorded on BRUKER AVIII500M (Bruker, Switzerland). B-NMR were recorded on JNM-ECZ500R/M1 (JEOL, Japan). Transmission electron microscopy (TEM) images were recorded on Talos L120C (Thermo Scientific, USA). Scanning electron microscope (SEM) images were recorded on Nova Nano 450 (Thermo Scientific, USA). The animal images were taken via an IVIS spectrum (PerkinElmer, USA). The fluorescent images were taken via a fluorescence microscope (T1, Nikon, Japan). Immunofluorescence images were recorded on a Laser Scanning Confocal Microscope (ECLIPSE Ti2, Nikon, Japan). The H&E, M&T, and immunohistochemistry images were collected via the digital slice scanner VS200 (Olympus, Japan).
Data analysis	All statistical analyses were performed on Graphpad Prism (version 8). MestReNova 7 was used for NMR analysis. AUC was calculated using the software Originlab 2018. Immunofluorescence staining: NIS-Elements Viewer (version 5.21). H&E, M&T, and immunohistochemistry staining: Olympus Image Viewer. Statistical analysis of immunohistochemistry: ImageJ2 (Fiji). The raw MS files of Glu-insulin were analysed and searched against the target protein database based on the species of the samples using Byonic.

For manuscripts utilizing custom algorithms or software that are central to the research but not yet described in published literature, software must be made available to editors and reviewers. We strongly encourage code deposition in a community repository (e.g. GitHub). See the Nature Portfolio guidelines for submitting code & software for further information.

Data

Policy information about availability of data

All manuscripts must include a data availability statement. This statement should provide the following information, where applicable:

- Accession codes, unique identifiers, or web links for publicly available datasets
- A description of any restrictions on data availability
- For clinical datasets or third party data, please ensure that the statement adheres to our policy

The authors declare that all of the data supporting the findings of this study are available within the paper and its Supplementary Information. Source data for the figures are provided with this paper.

Human research participants

Policy information about studies involving human research participants and Sex and Gender in Research.

Reporting on sex and gender	The study did not involve human research participants.
Population characteristics	—
Recruitment	—
Ethics oversight	—

Note that full information on the approval of the study protocol must also be provided in the manuscript.

Field-specific reporting

Please select the one below that is the best fit for your research. If you are not sure, read the appropriate sections before making your selection.

☒ Life sciences ☐ Behavioural & social sciences ☐ Ecological, evolutionary & environmental sciences

For a reference copy of the document with all sections, see nature.com/documents/nr-reporting-summary-flat.pdf

Life sciences study design

All studies must disclose on these points even when the disclosure is negative.

Sample size	Sample sizes were determined on the basis of a pilot study or of previous experimental experience. The in vitro studies were repeated at least three times independently, and in vivo experiments with five mice or three minipigs per group were performed.
Data exclusions	No data were excluded.
Replication	The experimental findings were reliably reproduced three times.
Randomization	All samples and organisms were randomly allocated into experimental groups.
Blinding	No formal blinding was used. In both the test and control groups, the experimental conditions and observed phenomena would reveal the type of treatment administered to the treated animals, rendering the conditions unsuitable for a double-blind experiment. Furthermore, blood-glucose monitoring is conducted using blood-glucose meters and CGMS, ensuring that subjective alterations do not affect the measurements.

Reporting for specific materials, systems and methods

We require information from authors about some types of materials, experimental systems and methods used in many studies. Here, indicate whether each material, system or method listed is relevant to your study. If you are not sure if a list item applies to your research, read the appropriate section before selecting a response.

Materials & experimental systems

n/a	Involved in the study
☐	☒ Antibodies
☐	☒ Eukaryotic cell lines
☒	☐ Palaeontology and archaeology
☐	☒ Animals and other organisms
☒	☐ Clinical data
☒	☐ Dual use research of concern

Methods

n/a	Involved in the study
☒	☐ ChIP-seq
☒	☐ Flow cytometry
☒	☐ MRI-based neuroimaging

Antibodies

Antibodies used

The following primary antibodies were used for IHC. They are listed as antigen first, followed by supplier (catalogue number).
1) Anti-Mouse TNFα, Rabbit anti-mouse antibody, Polyclonal, Immunoway (Cat # YT4689, 1:200).
2) Anti-Mouse IL6, Rabbit anti-mouse antibody, Polyclonal, Afinity (Cat # DF6087, 1:100).
3) Anti-Mouse IL10, Rabbit anti-mouse antibody, Polyclonal, Afinity (Cat # DF6894, 1:100).
4) Anti-Mouse IL12A, Rabbit anti-mouse antibody, Polyclonal, Afinity (Cat # AF5133, 1:100).
5) Anti-Mouse IL17A, Rabbit anti-mouse antibody, Polyclonal, Afinity (Cat # DF6127, 1:100).

The following primary antibodies were used for IF. They are listed as antigen first, followed by supplier (catalogue number).
1) Anti-alpha smooth muscle Actin, Mouse anti-mouse antibody, Monoclonal, Abcam (Cat # ab240654, 1:50000).
2) Anti-F4/80, Rabbit anti-mouse antibody, Monoclonal, Abcam (Cat # ab300421, 1:5000).
3) Anti-rabbit IgG (Alexa Fluor® 488 Conjugate), Goat anti-rabbit antibody, Cell signaling (Cat # 4412, 1:1000).
4) Anti-mouse IgG (Alexa Fluor® 594 Conjugate), Goat anti-mouse antibody, Cell signaling (Cat # 8890, 1:1000).

The following primary antibodies were used for WB. They are listed as antigen first, followed by supplier (catalogue number).
1) Anti-Phospho-Akt (Ser473), Rabbit anti-human antibody, Monoclonal, Cell signaling (Cat # 4060, 1:2000).
2) Anti-Akt (pan), Rabbit anti-human antibody, Monoclonal, Cell signaling (Cat # 4691, 1:1000).
3) Anti-β-Actin, Rabbit anti-human antibody, Polyclonal, Diagbio (Cat # db7283, 1:1000).
4) HRP AffiniPure Goat Anti-Rabbit IgG (H+L), Polyclonal, HANGZHOU FUDE (Cat # FDR007, 1:10000).

Validation

All antibodies used were from commercial sources and they can be verified through the item number on the antibody website.

Eukaryotic cell lines

Policy information about cell lines and Sex and Gender in Research

Cell line source(s)

HepG2 cells were obtained from the National Collection of Authenticated Cell Cultures (Shanghai, China).

Authentication

The identities of the cell lines were frequently checked by their morphological features, but were not authenticated by short tandem repeat (STR) profiling.

Mycoplasma contamination

All cell lines tested mycoplasma-negative by the standard PCR method.

Commonly misidentified lines
(See ICLAC register)

No commonly misidentified cell lines were used.

Animals and other research organisms

Policy information about studies involving animals; ARRIVE guidelines recommended for reporting animal research, and Sex and Gender in Research

Laboratory animals

Male and female C57BL/6 mice (six-to-eight weeks) were purchased from Hangzhou Medical College. Male Bama minipigs (six months) were purchased from Shanghai Jiaqian Biotechnology Co., Ltd.. The mice were maintained with a standard diet in 12-h light and 12-h dark cycles, allowing free access to food and water during the experiment. The ambient temperature was 20–26°C and the relative humidity was 50%–70%.

Wild animals

The study did not involve wild animals.

Reporting on sex

The study used male mice and minipigs to avoid disruption of the female estrous cycle. Female mice were only used in skin-fibrosis studies, to avoid the effects of male fighting.

Field-collected samples

The study did not involve samples collected from the field.

Ethics oversight

All animal procedures were performed following the Guidelines for Care and Use of Laboratory Animals of Zhejiang University (Protocol No. ZJU20220299).

Note that full information on the approval of the study protocol must also be provided in the manuscript.